

## **Theoretical Issues in the Calculation of the Electrical Resistivity of Plasmas<sup>1</sup>**

**F. Perrot<sup>2,3</sup> and M. W. C. Dharma-wardana<sup>4</sup>**

---

We recall briefly how the Ziman theory of electrical conductivity, first proposed for solids and liquid metals, has been extended to the case of plasmas. The physical assumptions and parameters entering the formula are analyzed. A self-consistent model of electronic and ionic structure of plasmas is then described and applied to the calculation of the resistivity. Results obtained for aluminum are shown and compared to measurements done by Benage, along a thermodynamic path going from normal density at melting to 0.03 compression at 41 eV. The important differences between theory and experiment are discussed. The uncertainties inherent to the theory are emphasized, and physical effects not taken into account in the theory are discussed. Finally, the need for accurate measurements is emphasized.

---

**KEY WORDS:** aluminum; average atom model; plasma conductivity; resistivity; Ziman theory.

### **1. INTRODUCTION**

The fast development of new experiments requiring numerical magneto-hydrodynamic simulations prompts studies of the electrical resistivity of materials in wide domains of densities and temperatures. Conductivity measurements in plasma state are extremely scarce so that the theoretical approach is in many cases the unique tool available in this kind of study. The first attempt to set up complete theoretical tables of conductivities was

---

<sup>1</sup> Paper presented at the Fifth International Workshop on Subsecond Thermophysics, June 16–19, 1998, Aix-en-Provence, France.

<sup>2</sup> Commissariat à l'Énergie Atomique, Centre d'Études de Bruyères-le-Châtel, BP No. 12, 91680 Bruyères-le-Châtel, France.

<sup>3</sup> To whom correspondence should be addressed.

<sup>4</sup> Institute for Microstructural Sciences, National Research Council, Ottawa K1A 0R6, Canada.

described by Rinker in 1985 [1]. Comparison of these data with experiments done later, as well as with other theoretical efforts, show the uncertainties inherent in these methods. Although more elaborate theories do exist, the systematic calculation of the resistivity requires a rather simple model. The only one that is sufficiently general is based on the Ziman theory [2], extended to liquid metals and plasmas [3]. In the present work, we recall this theory and show the difficulties in its application to plasmas. Results of numerical calculations are shown and compared with a few experimental points. We then comment on possible improvements of the theory.

## 2. ZIMAN THEORY IN PLASMAS

In plasmas, the extension of the Ziman theory of the resistivity [3], obtained from a variational solution of the linearized Boltzmann equation, leads to the expression

$$R = R_o \left( \frac{1}{n_e a_o^3} \right) \left( \frac{\tau_o}{\tau} \right) \quad (1)$$

where  $R_o = \hbar a_o / e^2$  is a reference resistivity ( $21.74 \mu\Omega \cdot \text{cm}$ ) with  $\hbar$  the Planck constant,  $a_o$  the Bohr radius, and  $e$  the electron charge. In Eq. (1),  $n_e$  is the electron density,  $\tau$  is the relaxation time, and  $\tau_o = 4\pi\epsilon_o \hbar a_o / e^2$  is a characteristic time. The relaxation time is related to the differential cross section for elastic scattering  $\Sigma(q, k)$ :

$$\frac{\tau_o}{\tau} = \frac{a_o^2}{3\pi Z^*} \left\langle \int_0^{2k} q^3 \Sigma(q, k) S(q) dq \right\rangle_e \quad (2)$$

The cross section depends on the momentum  $\mathbf{k}$  of the conduction electron before scattering and the transfer of momentum  $\mathbf{q}$  in the scattering event. The electron energy is

$$\epsilon = \frac{\hbar^2 k^2}{2m} \quad (3)$$

and the momentum transfer:

$$q = k(1 - \cos \theta)^{1/2} \quad (4)$$

with  $\theta$  the angle between  $\mathbf{k}$  and  $\mathbf{k} + \mathbf{q}$ . In Eq. (2),  $\Sigma(q, k)$  is relative to a single-scattering plasma ion. The total scattering for the whole plasma is obtained by

multiplying by the ionic structure factor  $S(q)$ . This is a superposition approximation assuming that the scattering ions act independently and is justified when the electronic structure is comparable to that of simple metals or, equivalently, when the pseudopotential theory for weak electron-ion interactions is applicable. The bracket in Eq. (2) indicates averaging over the energy of the conduction electron:

$$\langle g(\varepsilon) \rangle_\varepsilon = - \int_0^\infty d\varepsilon \frac{df(\varepsilon)}{d\varepsilon} g(\varepsilon) \quad (5)$$

where a free electron density of states is assumed, and  $f(\varepsilon)$  is the Fermi-Dirac distribution appropriate to the density-temperature conditions. The last important quantity present in Eq. (2) is the effective number of free electrons per plasma ion  $Z^*$ . This quantity is well defined for simple metals but can lead to serious difficulties in transition metals or in dense plasmas.

### 3. CALCULATIONS IN PLASMAS

The quantities entering the Ziman formula are obtained from a first-principles model dealing with the calculation of both the electronic and the ionic structures.

#### 3.1. Average Atom Electronic Structure

The electronic structure model belongs to the family of average atom models (AAM) based on the density functional theory (DFT) proposed by Hohenberg and Kohn [4] and Kohn and Sham [4] for electronic systems in their ground state, and extended to thermal equilibrium ensembles by Mermin [5]. Our application of this theory [6] gives the electron charge density  $n(r)$  around a bare nucleus embedded in an electron gas of density  $n_e$ , originally uniform. The electron gas is neutralized by a background of positive charge (jellium) containing a spherical cavity of radius equal to the atomic radius  $r_a$ , with the nucleus of charge  $Z$  at its center. The ionic density is

$$n_i = \frac{1}{(4/3) \pi r_a^3} \quad (6)$$

and the density of the uniform electron gas is related to  $Z^*$  mentioned above by

$$n_e = Z^* n_i \quad (7)$$

The nucleus induces a pile up of screening electronic charge. The quantum mechanical self-consistent solution relies on the techniques proposed by Friedel for solving the impurity problem [7, 8] in which the phase shifts of continuum wave functions play an important role. Details on these techniques and their extension to finite temperatures can be found elsewhere [9, 10]. The relaxed electron charge density is written:

$$n(r) = n_b(r) + \Delta n_f(r) + n_e \quad (8a)$$

$$n_b(r) = \sum_b g_b f_b |\varphi_b(r)|^2 \quad (8b)$$

$$\Delta n_f(r) = \frac{2}{(2\pi)^3} \int_0^\infty f_k d^3k \sum_l 2(2l+1)(|\varphi_{l,k}(r)|^2 - |j_l(kr)|^2) \quad (8c)$$

$n_b(r)$  is the bound charge density, a sum over all the bound states  $b$ , with degeneracy  $g_b$  and wavefunction  $\varphi_b(r)$ , existing in the self-consistent potential. Equation (8c) gives the contribution of the continuous spectrum as an integral over all the free electron energies [see Eq. (3)] and a sum over angular momenta. The free wave functions are normalized to Bessel functions  $j_l(kr)$  at infinity. The occupation numbers  $f_b$  and  $f_k$  are given by Fermi-Dirac statistics. The electron density  $n(r)$  is characteristic of an AAM in the sense that the electron states are populated with a noninteger number of electrons. It can be interpreted as a thermal average of all the actual configurations with integer populations that exist in the plasma. A multiple-ion model going beyond the AAM is discussed in Section 5. The total number of bound electrons is easily deduced from Eq. (8b), so that the number of free electrons is

$$Z^* = Z - \sum_b g_b f_b \quad (9)$$

depending on density and temperature. Such a definition can lead to difficulties in the case of strong pressure ionization [10], but we do not discuss this point here.

### 3.2. Pseudopotential and Ionic Structure

The next step in the resistivity calculation is the definition of the ion-ion interaction that determines the ionic structure. The assumption of a pair interaction is made. This is certainly a good approximation in simple metals (by definition) and in plasmas when those conduction electron states which play a role in metallic binding are of  $s$  and  $p$  symmetry and

feel a rather weak ion core potential. In more complex cases, when the electron-ion interaction is strong due to the lack of core states orthogonalization (for instance in hydrogen), or when high angular momenta are involved (transition metals, rare earths, actinides, etc.), the pair-interaction assumption breaks down. Let us note also that, in most plasmas of simple metals, there exist domains of temperature and density where the electronic structure becomes complex: this happens when localization of a bound state occurs because the density decreases or the temperature increases. Such situations will be found for aluminum in Section 4. We define the pseudopotential, when justified, as

$$w(q) = \frac{\Delta n_f(q)}{\Pi(q)} \quad (10)$$

where  $\Delta n_f(q)$  is the Fourier transform of the AAM density of the continuum states given in Eq. (8b) and  $\Pi(q)$  is the interacting density-response function of a uniform electron gas at density  $n_e$  and temperature  $T$ . Some attention must be paid in subtracting the oscillations of the charge density inside the ionic core. The temperature and density dependent  $w$  of Eq. (10) behaves, in coordinate space, like  $-Z^*/r$  at large distances. Using standard pseudopotential theory, the pair interaction takes the form

$$\Phi(q) = \frac{4\pi(Z^*e)^2}{q^2} + w(q) \Delta n_f(q) \quad (11)$$

Once the pair interaction is defined, the ionic structure of the plasma can be determined. The pair distribution function  $g(r)$  is a solution of one of the integral equations well known in the theory of classical fluids. We use the hypernetted-chain (HNC) theory or its improvement, the modified HNC (MHNC) theory [11], which is better when ion coupling is strong. The Fourier transform of  $g(r) - 1$  gives  $S(q)$  in Eq. (2).

### 3.3. Elastic Scattering Cross Section

The Ziman formula has been widely applied to calculations in simple liquid metals [12] with some success. In plasmas, it has been used in conjunction with more or less sophisticated models of electronic and ionic structure [1, 13–16]. An important issue in these calculations is the determination of the cross section.  $\Sigma(q, k)$  can be calculated either with the (local) pseudopotential formulation (independent of  $k$ ),

$$\Sigma_{ps}(q) = \frac{1}{4\pi^2} \frac{m^2}{\hbar^4} \left( \frac{w(q)}{\mathcal{E}(q)} \right)^2 \quad (12)$$

where  $\mathcal{E}(q)$  is the dielectric function, or, alternatively, from the scattering amplitudes,

$$\Sigma_{sc}(q, k) = \frac{1}{k^2} \left| \sum_l (2l+1) e^{i\delta_l(k)} \sin(\delta_l(k)) P_l(\cos \theta) \right|^2 \quad (13)$$

in terms of the wave-function phase shifts  $\delta_l(k)$ . When the electron-ion interaction is really weak, the two formulations give the same result. But for di- or trivalent simple metals, the difference can be significant. In the case of a strong interaction, the second formulation, Eq. (13), should be better since it does not require linear response to the potential. It is puzzling to see that this is not the case, for example, in aluminum. In Table I, we compare the values of the resistivity at constant electron density  $n_e = 0.027$  atomic unit (i.e. the electron density in normal solid aluminum), obtained from the two cross-section formulas. The phase-shift cross section gives a much larger value of the resistivity. The pseudopotential cross section is in much closer agreement with experiment at low temperatures: the resistivity measured in liquid aluminum at melting is  $R = 24.4 \mu\Omega \cdot \text{cm}$ . The strong disagreement between the two calculations may be due to the following reasons. (i) When the two cross sections differ strongly, then the exact density of states also differs strongly from the free electron density of states. The exact one, calculated from the phase shifts should be used as a weight factor in the averaging of Eqs. (2) and (5). It should also be noted that if the pseudopotential is defined via Eq. (10), then the correct density of states is, in a sense, automatically folded into  $w(q)$ , thus improving the quality of the pseudopotential calculation. (ii) The single (i.e., isolated) scatterer assumption contained in the convolution with  $S(q)$  may not be

**Table I.** Comparison of the Resistivities Calculated in Aluminum, at Constant Electron Density and Increasing Temperature, with Two Possible Formulations of the Cross Section: The Number of Free Electrons Is Also Shown

$T$ (eV)	$Z^*$	$R_{ps}$ ( $\mu\Omega \cdot \text{cm}$ )	$R_{sc}$ ( $\mu\Omega \cdot \text{cm}$ )
2.5	3.000	26.6	115
5	3.000	38.3	122
10	3.023	71.5	150
20	3.600	121	182
30	4.348	141	182
40	5.193	136	167
60	6.306	122	149
80	7.233	109	128
100	8.272	96.2	111

valid. If the atomic-ordering length scale in the plasma becomes of the order of some of the  $k$ -dependent electron mean free paths, or if multicenter resonances exist in the spectrum, the multiple scattering effects beyond the convolution model become relevant. Their full treatment, impossible in the framework of simple models, would be the key to the problem in these cases.

## 4. COMPARISON WITH EXPERIMENT

### 4.1. Measurements in Liquid Metals

Many experimental results on the resistivity of metals at melting are available [12]. But few experiments give the resistivity as a function of temperature. Let us note, for example, the measurements of Al, Ge, and Al-Ge alloys at normal pressure [17]. Experiments under pressure are also reported by the CEA team: for tantalum and tungsten [18] and more recently, for beryllium [19], uranium [20], cerium [21], rhenium [22], and thorium [23] using the isobaric expansion technique.

### 4.2. Plasmas

In dense plasmas, one of the earliest resistivity measurements using the exploded wire technique was due to Shepherd et al. [24], for polyurethane, at a temperature of 10 eV and an electron density of about  $6 \times 10^{22} \text{ e} \cdot \text{cm}^{-3}$ . Unfortunately, these measurements were not very accurate. More recently, the same technique was used by DeSilva and Kunze [25] in copper plasmas, between 1 and 3 eV, and in the range of 0.5 to 2  $\text{g} \cdot \text{cm}^{-3}$ . New experiments on polyurethane are reported by Benage [26], at higher temperatures (25 to 30 eV) and for a density of  $1.265 \times 10^{-2} \text{ g} \cdot \text{cm}^{-3}$ .

The measurement of resistivity along a thermodynamic path going from the melting point under normal conditions to a state corresponding to a compression of 0.03 at  $T=41 \text{ eV}$  in Al has been performed at Los Alamos by Benage [27], using the exploding wire method. The density, temperature, and resistivity are given for 14 points along the path. In Fig. 1, we show the temperature as a function of density, as estimated by Benage in a numerical simulation using the Sesame equation of state [28]. The ionization  $Z^*$  calculated with the theoretical model of Section 3 is also plotted. The curve presented is continuous, although there exist densities where the calculation is meaningless because a bound state is crossing the onset of localization. The highest existing bound states are indicated on the curve. In Fig. 2, we compare experimental values with the theoretical

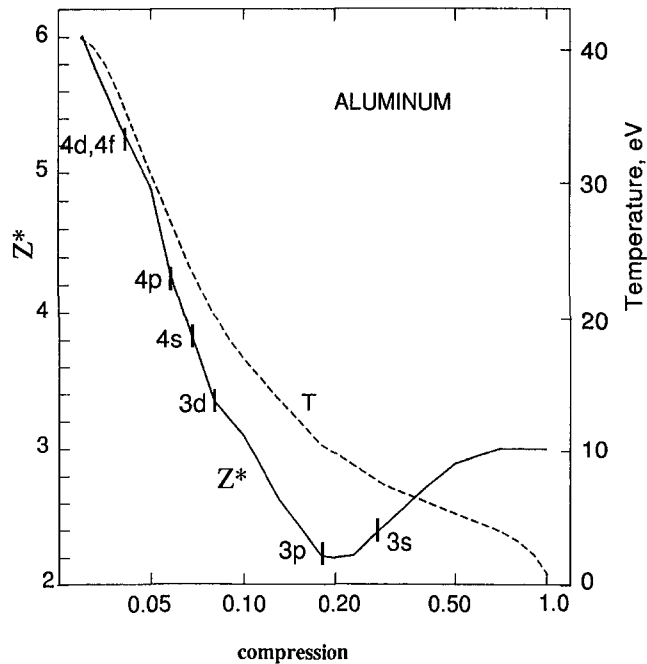


Fig. 1. Temperature (dashed curve) along the thermodynamic path of the experiment in aluminum done at Los Alamos by Benage [27], and the average number of free electrons  $Z^*$ , calculated with the AAM (solid curve). The highest bound state existing in the AAM, at a given temperature-density point, is indicated along the curve.

resistivities obtained with the phase shifts and the free-electron density of states averaging, and with the pseudopotential.

The discrepancy between theoretical estimates themselves, and between theory and experiment is very important. Unfortunately, the experimental error bars are not available. In addition, one must keep in mind that the temperature is not measured, but results from a simulation. Also, the diameter of the plasma column in the exploding wire may vary along the wire and during the measurement. For the theoretical calculations, we can make the following comments. (i) The structure factor  $S(q)$  is important at low temperature only ( $T < 10$  eV). Thus, if it is assumed that Eqs. (1) and (2) are correct, the uncertainties on this quantity play a minor role. (ii) The cross section is crucial. The pseudopotential formulation gives good results at normal density, but deviates from experiment for compressions lower than 0.2. On the other hand, the phase shift formulation overestimates the resistivity at normal density, but gives values that are of the right order of



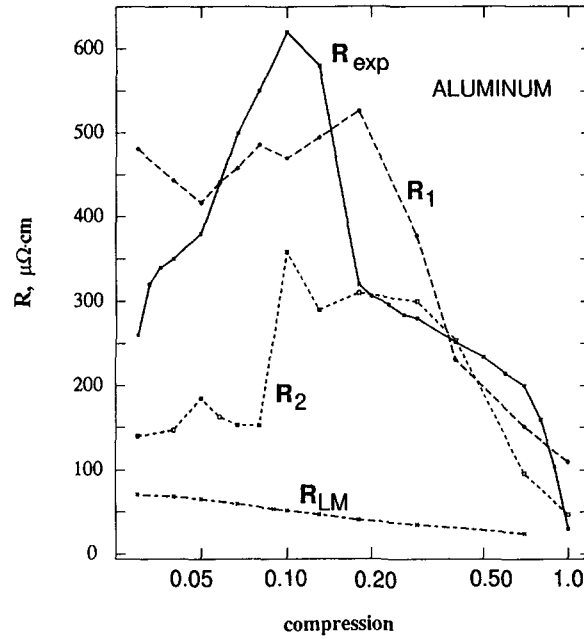


Fig. 2. Electrical resistivity in the aluminum plasma of the Benage experiment.  $R_{\text{exp}}$  is the measured value.  $R_1$  and  $R_2$  are calculated using the phase-shift and pseudopotential formulations of the scattering cross section, respectively.  $R_{\text{LM}}$  is the corresponding calculation using the Lee and More model [30].

magnitude at low compression and high temperature, even if the accuracy is poor. The Spitzer formula [29], frequently used in classical plasmas, gives  $R = 245 \mu\Omega \cdot \text{cm}$  for a compression of 0.1. In Fig. 2 we have also plotted the results of the simple theory proposed by Lee and More [30].

## 5. POSSIBLE IMPROVEMENTS IN THE THEORY

### 5.1. Beyond the Average Atom Model

The question of the adequacy of the AAM for the resistivity calculation must be considered.  $Z^*$  is the appropriate parameter relating the electron and ion densities in Eqs. (6) and (7). But the cross section is not obviously related to  $Z^*$ . Let us think of the plasma as an assembly of ions of various charge  $Z_i^*$ . In the pseudopotential formulation, we have

$$\Sigma_{ps}(q) = \frac{1}{4\pi^2} \frac{m^2}{\hbar^4} \sum_{i,j} x_i x_j S_{ij}(q) \frac{w_i(q) w_j(q)}{\mathcal{E}(q) \mathcal{E}(q)} \quad (14)$$

**Table II.** Comparison of the Resistivities in Aluminum, as Calculated Using the Multiple-Ion Model (MIM) or the Average Atom Model (AAM), with the Pseudopotential Formulation of the Cross Section

$T$ (eV)	Compression	$R_{ps}$ ( $\mu\Omega \cdot \text{cm}$ )	
		MIM	AAM
5	0.1	810	405
5	0.2	720	590
5	0.3	490	318
5	0.4	312	240
5	0.5	203	165
10	0.2	382	288
10	0.3	296	240
10	0.4	220	220
10	0.5	164	164

where  $w_i(q)$  is the pseudopotential of ionic species  $i$  with ionic charge  $Z_i^*$  and concentration  $x_i$ . The partial structure factors are  $S_{ij}(q)$  obtained by solving coupled integral HNC equations, with pair interactions built using the pseudopotentials. Table II shows a comparison, in aluminum, between calculations done in this multiple ion model (MIM) [31] and in the AAM of Section 3. The MIM resistivities are larger, except when the conditions are such that there is only one ionic species in the plasma ( $T = 10$  eV for compressions of 0.4 and 0.5). If we take the trends of Table II into account, the curve  $R_2$  in Fig. 2 must be shifted up, in better agreement almost everywhere with experiment. This clearly calls for more detailed MIM calculations in order to interpret this experiment. Unfortunately, these calculations become more and more difficult when the number of relevant configurations increases at high temperatures.

## 5.2. Effect of Inelastic Contributions to Scattering

When the bound spectrum of an atom contains levels which are rather close in energy, the scattering of an incident electron may be accompanied by the transition of a core electron from one of these bound states to another. The scattering becomes inelastic. Such a process has already been suggested in different circumstances [32]. It can change the resistivity. In the analysis starting with the Boltzmann equation, the rate of change

$$\frac{\Delta f(\mathbf{k})}{\tau(\mathbf{k})} = \frac{f(\mathbf{k}) - f_o(\mathbf{k})}{\tau(\mathbf{k})} \quad (15)$$

in the momentum distribution of the conduction electron due to the electric field can be estimated with the help of the Fermi Golden Rule. The inelastic scattering of the incident electron  $e$  by a core electron  $c$  is associated with the Coulomb interaction  $\Delta H = e^2/r_{ce}$ , so that the relevant matrix element is

$$\begin{aligned} \langle ik | \Delta H | jk' \rangle &= \frac{1}{\Omega} \int \varphi_i^*(\mathbf{r}_c) \varphi_j(\mathbf{r}_c) \frac{e^2}{r_{ce}} e^{-i(\mathbf{k}-\mathbf{k}') \cdot \mathbf{r}_c} d^3r_c d^3r_e \\ &= \frac{1}{\Omega} \frac{4\pi e^2}{q^2} \langle i | e^{i\mathbf{q} \cdot \mathbf{r}} | j \rangle \end{aligned} \quad (16)$$

where  $\mathbf{k}$  and  $\mathbf{k}'$  are the momenta of the incident electron before and after scattering. The wave functions for the conduction states have been assumed to be plane waves, normalized in the volume  $\Omega$  of the plasma. The bound states occupied by the core electron  $c$  before and after the collision are  $i$  and  $j$ , and  $\mathbf{q} = \mathbf{k}' - \mathbf{k}$  is the momentum transfer. The energy conservation can be expressed as

$$k'^2 = k^2 + \frac{2m}{\hbar^2} (\varepsilon_i - \varepsilon_j) \quad (17)$$

Using this matrix element in the Golden Rule for the rate of transition, we obtain, after some algebra,

$$\begin{aligned} \frac{\tau(k)}{\tau_{el}(k)} &= 1 + \frac{n_i}{2\pi} \sum_{i \neq j} f_i (1 - f_j) \frac{1 - f_o(k')}{1 - f_o(k)} k'^2 \\ &\quad \times \int_0^\pi F_{ij}(q) \sin \theta d\theta \left( \frac{k' \tau(k')}{k \tau(k)} \cos \theta - 1 \right) \end{aligned} \quad (18a)$$

$$F_{ij}(q) = \frac{1}{(2l_i + 1)(2l_j + 1)} \sum_{m_i, m_j} \left| \frac{4\pi e^2}{q^2} \langle i | e^{i\mathbf{q} \cdot \mathbf{r}} | j \rangle \right|^2 \quad (18b)$$

where  $\theta$  is the angle between  $\mathbf{k}$  and  $\mathbf{k}'$ . For each pair  $i$  and  $j$ ,  $k$  and  $k'$  are related by Eq. (17).  $n_i$  is the ionic density; and  $f_i$  and  $f_j$  are the equilibrium populations of the core states. The total relaxation time  $\tau(k)$  couples with the elastic relaxation time  $\tau_{el}(k)$  and with the total relaxation time for  $k'$ . The structure of Eq. (18a) is complex and, up to now, we have no formal solution of it. It can be simplified if the inelastic contribution is not too large. Numerical calculations along these lines are in progress. Significant changes in the calculated resistivity can be expected.

## 6. CONCLUSION

We have shown that the systematic calculation of the resistivity in plasmas, even in the framework of a simple theory, is a difficult task. It would be much more complicated in plasmas of heavy elements, where both the electronic and the ionic structure are not well understood. The problem of how to treat the multiple scattering of an electron by the plasma ions is certainly at the heart of the problem. Furthermore, the question of the adequacy of the simple average atom model is not clearly answered. The change of the energy scale of the relevant processes when the temperature rises might require accounting for inelastic scattering effects. Anyway, measurements of the resistivity of plasmas in wide domains of temperatures and densities are needed. Provided the plasma parameters and the resistivity are measured with a known accuracy, they will provide tests of the physical assumptions in the theoretical models. Experiments using isobaric vessel techniques seem promising. Another type of experimental method, measuring the plasma reflectivity, has been described in the literature [33]. It could, in principle, explore wider domains of temperatures but, up to now, leads to difficult interpretations [34]. Nevertheless, there is no doubt that the study of transport properties of plasmas will develop very fast in the near-future.

## REFERENCES

1. G. Rinker, *Phys. Rev. B* **31**:4207 (1985).
2. J. M. Ziman, *Electrons and Phonons*, N. F. Mott, E. C. Bullard, and D. H. Wilkinson, eds. (Clarendon, Oxford, 1960), p. 220.
3. R. Evans, B. L. Gyorffy, N. Szabo, and J. M. Ziman, *The Properties of Liquid Metals*, S. Takeuchi, ed. (Wiley, New York, 1973), p. 319.
4. P. Hohenberg and W. Kohn, *Phys. Rev. B* **136**:864 (1964); W. Kohn and L. J. Sham, *Phys. Rev. A* **140**:1133 (1965).
5. N. D. Mermin, *Phys. Rev. A* **137**:1441 (1965).
6. M. W. C. Dharma-wardana and F. Perrot, *Density Functional Theory*, E. K. U. Gross and R. M. Dreizler, eds. (Plenum, New York, 1995).
7. J. Friedel, *Philos. Mag.* **43**:153 (1952); *Adv. Phys.* **3**:446 (1954).
8. L. Dagens, *J. Phys. (Paris)* **34**:879 (1973); *J. Phys. C* **5**:2333 (1972).
9. F. Perrot, *Phys. Rev. A* **25**:489 (1982).
10. F. Perrot, *Phys. Rev. A* **42**:4871 (1990); *Phys. Rev. A* **47**:570 (1993).
11. F. Lado, S. M. Foiles, and N. W. Ashcroft, *Phys. Rev. A* **28**:2374 (1983).
12. M. Shimoji, *Liquid Metals* (Academic, London, 1977), p. 254.
13. H. Minoo and C. Deutsch, *Phys. Rev. A* **14**:840 (1976).
14. D. B. Boercker, F. J. Rogers, and H. E. DeWitt, *Phys. Rev. A* **25**:1623 (1982).
15. S. Ichimaru and S. Tanaka, *Phys. Rev. A* **32**:1790 (1984).
16. F. Perrot and M. W. C. Dharma-wardana, *Phys. Rev. A* **36**:238 (1987).
17. J. G. Gasser, M. Mayoufi, and M. C. Bellisent-Funel, *J. Phys. Condens. Matter* **1**:2409 (1989).

18. A. Berthault, L. Arlès, and J. Matricon, *Int. J. Thermophys.* **7**:167 (1986).
19. M. Boivineau, L. Arlès, J. M. Vermeulen, and Th. Thévenin, *Int. J. Thermophys.* **14**:427 (1993).
20. M. Boivineau, L. Arlès, J. M. Vermeulen, and Th. Thévenin, *Physica B* **190**:31 (1993).
21. M. Boivineau, J. B. Charbonnier, J. M. Vermeulen, and Th. Thévenin, *High Temp.-High Press.* **25**:311 (1993).
22. Th. Thévenin, L. Arlès, M. Boivineau, and J. M. Vermeulen, *Int. J. Thermophys.* **14**:441 (1993).
23. M. Boivineau, H. Colin, J. M. Vermeulen, and Th. Thévenin, *Int. J. Thermophys.* **17**:1001 (1996).
24. R. L. Shepherd, D. R. Kania, and L. A. Jones, *Phys. Rev. Lett.* **61**:1278 (1988).
25. A. W. DeSilva and H. J. Kunze, *Phys. Rev.* **E61**:4448 (1994).
26. J. F. Benage, Jr., W. R. Shanahan, E. G. Sherwood, L. A. Jones, and R. J. Trainor, *Phys. Rev.* **E49**:4391 (1994).
27. J. F. Benage, Jr., personal communication (Los Alamos National Laboratory, Los Alamos, NM, 1995).
28. W. F. Huebner, *T-4 Handbook of Material Properties Data Bases, Vol. 1c. Equations of State*, K. S. Holian, ed. (Los Alamos National Laboratory, LA-10160-MS, Los Alamos, NM, 1984).
29. L. Spitzer and R. Härm, *Phys. Rev.* **89**:977 (1953).
30. Y. H. Lee and R. M. More, *Phys. Fluids* **27**:1273 (1984).
31. F. Perrot and M. W. C. Dharma-wardana, *Phys. Rev.* **E52**:5352 (1995).
32. O. Entin-Wohlman and Y. Imry, *Phys. Rev. B* **45**:1590 (1992).
33. H. M. Milchberg, R. R. Freeman, S. Davey, and R. M. More, *Phys. Rev. Lett.* **61**:2364 (1988); A. N. Mostovych and Y. Chan, *Phys. Rev. Lett.* **79**:5094 (1997).
34. A. Ng, P. Celliers, F. Perrot, M. W. C. Dharma-wardana, R. M. More, Y. H. Lee, and G. Rinker, *Phys. Rev. Lett.* **72**:681 (1994); M. W. C. Dharma-wardana and F. Perrot, *Phys. Lett. A* **163**:223 (1992).